# Fabrication of the 7.3 m long coils for the prototype of MQXFB, the $Nb_3Sn$ low-b quadrupole magnet for the HiLumi LHC

F. Lackner, P. Ferracin, G. Ambrosio, E. Todesco, M. Duret, S. Triquet, M. Pozzobon, S. Luzieux, J.C. Perez, C. Scheuerlein, T. Sahner, M. Michels, M. Semeraro, N. Bourcey, E. Cavanna, P. Revilak, T. Genestier, J. Axensalva, R. Principe, H. Prin, F. Savary

***Abstract*— The High luminosity LHC upgrade target is to increase the integrated luminosity by a factor 10, resulting in an integrated luminosity of 3000 fb-1. One major improvement foreseen is the reduction of the beam size at the collision points. This requires the development of 150 mm single aperture quadrupoles for the interaction regions. These quadrupoles are under development in a joint collaboration between CERN and the US-LHC Accelerator Research Program (LARP). The chosen approach for achieving a nominal quadrupole field gradient of 132.6 T/m is based on the $Nb_3Sn$ technology. The coils with a length of 7281 mm will be the longest $Nb_3Sn$ coils fabricated so far for accelerator magnets. The production of the long coils was launched in 2016 based on practise coils made from copper. This paper provides a status of the production of the first low grade and full performance coils and describes the production process and applied quality control. Furthermore an outlook for the prototype assembly is provided.**

***Index Terms*— High Large Hadron Collider (LHC), Low-β Quadrupoles, $Nb_3Sn$ magnets, long prototype, support structure, Large Magnet Facility (LMF).**

## I. Introduction

IN the period 2015-2023, the LHC is expected to reach a peak luminosity of $2 \cdot 10^{34}$ $cm^{-2}s^{-1}$ with a possible increase of energy to 7 TeV per beam. As part of the HiLumi Project at CERN an upgrade of the interaction region in the period 2024-2026 is planned in order to achieve a peak luminosity of $5 \cdot 10^{34}$ $cm^{-2}s^{-1}$, and to reach 3000 $fb^{-1}$ integrated luminosity about 12 years after the upgrade [1]. The components to be upgraded include the inner triplet (or low-β) quadrupole magnets, named Q1, Q2a, Q2b, and Q3. These current triplet quadrupoles use Nb-Ti superconducting coils to generate a gradient of 215 T/m in a 70 mm aperture, with a magnetic length of 6.3 m for Q1 and Q3 [2], and 5.5 m for Q2a and Q2b [3], and with a conductor peak field of 7.7 and 8.6 T respectively. This inner triplet will be replaced by a new magnet type called MQXF. It is based on $Nb_3Sn$ technology allowing for an aperture of 150 mm, a peak field on the conductor of 11.4 T, operating at a gradient of 132.6 T/m. Two types of magnets will be produced. Two MQXFA with a magnetic length of 4.2 m will be using the cold mass and cryostat of the Q1 and Q3 quadrupoles. The MQXFB with a magnetic length of 7.15 m will be inserted in a single cold mass and the cryostat for the Q2a and Q2b. Two MQXFB magnet prototypes will be manufactured at the Large Magnet Facility (LMF) at CERN until 2019 [4-6].

## II. Status of the Coil Production

The production layout and major modifications to the previous Nb-Ti coil production as well as the coil winding and curing process were presented in [8]. In 2016 two copper practise coils were produced, followed by two coils made from low performance $Nb_3Sn$ RRP conductor. The production is currently continuing on the RRP full performance conductor. Table I represents the status of this coil production for the first prototype. The first full performance coil (CR103) was unfortunately lost after the reaction heat-treatment (RHT) due

TABLE I
Coil production for the assembly of the first MQXFB prototype

| Coil ID | Conductor | Status | Date |
|---|---|---|---|
| CR101 | RRP-low grade | Impregnated | March 2017 |
| CR102 | RRP-low grade | Impregnated | July 2017 |
| CR103 | RRP | Damage after RHT | June 2017 |
| CR104 | RRP | Wound and cured | July 2017 |
| CR105 | RRP | Wound and cured | August 2017 |
| CR106 | RRP | Cable received | August 2017 |
| CR107 | RRP | Cabling | August 2017 |

Fig. 1. Winding area in the Large Magnet Facility at CERN, bldg. 180.

This work was supported by the European Commission under the FP7 project HiLumi LHC under Grant GA 284404, co-funded by the DoE, USA and KEK, Japan.

F. Lackner is with CERN, Technology Department, 1211 Geneva 23, Switzerland, e-mail: Friedrich.Lackner@cern.ch.
P. Ferracin, E. Todesco, F. Savary, S. Triquet, M. Pozzobon, S. Luzieux, J.C. Perez, C. Scheuerlein, R. Principe, H. Prin, M. Duret, N. Bourcey, T. Sahner, M. Michels, M. Semeraro, J. Axensalva are with CERN, Technology Department, CH-1211 Geneva 23, Switzerland.
P. Revilak is with Babcock Noell GmbH, Wuerzburg, 97080 Germany.
T. Genestier is with General Electric, 90018 Belfort, France.
E. Cavanna is with ASG Superconductors S.p.A., Corso F.M. Perrone 73R, 16152 Italy.
G. Ambrosio is with Fermi National Accelerator Laboratory, Batavia, IL 80510 USA.

This document was prepared by LARP collaboration using the resources of the Fermi National Accelerator Laboratory (Fermilab), a U.S. Department of Energy, Office of Science, HEP User Facility. Fermilab is managed by Fermi Research Alliance, LLC (FRA), acting under Contract No. DE-AC02-07CH11359

to non-conform clamping of the cable in the splicing region throughout the RHT. The coil will however be impregnated in in 2017 and will be used as a practise coil for the first MQXFB test assembly.

Coil CR104 will be reacted in September 2017 followed by the vacuum impregnation. The winding and curing of coil CR105 have been launched in the beginning of August and will be finalized after the production duration of three working weeks. RHT for coil CR105 as well as the winding of coil CR106 and subsequently CR107 will be launched in September. The current production schedule will allow for delivery of four prototype coils in early 2018 followed by the assembly of the first full performance prototype. Figure 1 provides an overview of the CERN winding area located in the Large Magnet Facility (LMF). The working area was further optimized in 2017 and allows now to work in parallel with two sets of tooling for winding and reaction. In parallel to the coil fabrication the LMF quality assurance team has continuously improved the developed working procedures. In addition electrical and geometrical measurements carried out in line with the coil production will assure continuous monitoring of achieved quality.

## III. Geometrical and Electrical Coil Qualification

Regarding the geometrical qualification the distribution of the titanium pole gaps before winding operation is crucial to achieve a closed pole gap after the RHT. The titanium pole of the MQXFB coils is divided into seventeen parts which are assembled on the winding mandrel. A total gap width of 16 mm equally distributed between each pole was found to be the most adequate taking into account the variation of the pole gap during the following production steps:

- Release of winding tensions after winding and curing, when the coil is dismounted from the winding mandrel and transferred to the reaction fixture;
- Coil contraction during the RHT.

The gap between the pole pieces is measured prior and after the RHT. Table II shows the pole gap value measured before the

TABLE II
Total pole gap measured during steps of fabrication

| Coil ID | Before winding [mm] | Before heat treatment [mm] | After heat treatment [mm] |
|---|---|---|---|
| CR101 | 17.6 | 12.5 | 6.6 |
| CR102 | 17.6 | 10 | 1.8 |
| CR103 | 13.6 | 7.9 | 0 |
| CR104 | 16 | * | * |
| CR105 | 16 | * | * |

start of the winding operation. It also contains the values prior and after the RHT.

TABLE III
Contraction during steps of fabrication in mm/m

| Coil ID | Initial gap [mm/m] | Releasing winding tensions [mm/m] | After reaction heat treatment [mm/m] | Total contraction [mm/m] |
|---|---|---|---|---|
| CR101 | 2.50 | 0.72 | 0.84 | 1.56 |
| CR102 | 2.50 | 1.08 | 1.16 | 2.24 |
| CR103 | 1.93 | 0.81 | 1.12 | 1.93 |
| CR104 | 2.27 | | * | * |
| CR105 | 2.27 | | * | * |

Table III provides an overview of the measured pole gap in mm/m after each production step. As an example the pole gap for the coil CR101 of initially 2.5 mm/m is reduced to 0.72 mm/m when releasing the winding tension for assembly of the reaction fixture. After the RHT a remaining pole gap of 0.84 mm/m was measured which results in a total contraction of 1.56 mm/m. The optimization throughout the practise coil production has allowed to adjust these initial values in order to achieve a closed pole gap.

Each production step is followed by an electrical qualification test at low current. Table IV provides an overview on all tests applied. As can be seen the qualification is carried out based on

TABLE IV
Overview on electrical test for the MQXFB coil production

| Step | Note | R 2A | R 10A | L | C | Insulation |
|---|---|---|---|---|---|---|
| RHT fixture assembly | Fixture open | X | | X | | X |
| | Fixture closed | X | | X | X | X |
| | Fixture bolted | X | | X | X | X |
| After RHT | Fixture open | X | | X | | X |
| After splicing | | | X | | | |
| Trace setup | Outer trace | X | | X | | |
| | Inner trace | X | | X | | |
| Impregnation | Monitoring | | | | X | |
| | Fixture closed | X | | X | X | X |
| | Fixture open | X | | X | | |
| Final test | Coil only | X | | X | | X |

resistance measurements at low current of 2 A during the major construction steps. An exception is given by the qualification after the splicing of the $Nb_3Sn$ to Nb-Ti current leads which is

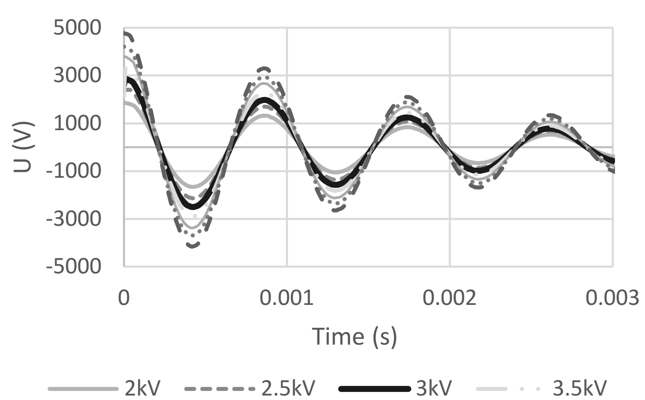


Fig. 2. Electrical discharge test up to 5 kV on the coil CR101.

carried out at 10 A. The inductance measurement is carried out to identify possible short cuts between the cable turns while the measurement of the inductance can provide information on the quality of the insulation layers. Figure 2 provides the plot of the measured discharge voltage test. This test is carried out after the coil impregnation as a final test at 2.5 kV. Coil CR101 was measured with 5 kV in order to verify the insulation limit between the cable turns. The successful result has underlined the robustness of the resin insulation. Figure 3 is presenting the electrical resistance measurement with a current of 2 A throughout the coil production. The reaction fixture assembly and bolting (assembly step 1 to 3) do not show a major impact on the resistance values. After the RHT (step 4) the coil resistance value is increasing which can be explained by the pollution of copper during the RHT. The geometrical qualification of the coil is carried out in the LMF winding zone. A 16 m long granite table with a planarity of 40 µm is available to carry out these measurements. The measurement device is a portable coordinate measuring machine [7]. For the coil

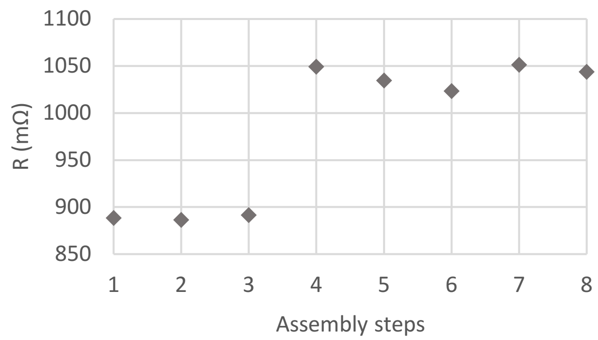


Fig. 3. Change of electrical resistance throughout production of the coil CR103, tests carried out as indicated in Table IV, test current 2A.

assembly the arc length is the value defining the required coil shimming. Figure 4 represents the deviation of the azimuthal coil size in mm. The cross-section is measured each 200 mm over the coil length. The graph shows a variation in the total arc length of up to 100 µm creating a minor asymmetry of

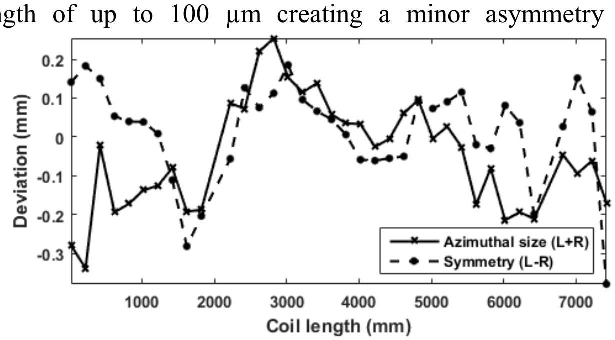


Fig. 4 Coil azimuthal size (mean value) versus coil length.

maximum 300 µm. This is given mainly by the assembly tolerances on the impregnation fixture. The applied metrology process and definition of shimming dimensions for both the short model magnets as well as the long prototype coils are presented in [7]

## IV. REACTION HEAT TREATMENT

The furnace GLO10000 was introduced in [8] and its successful commissioning described in [9]. It was specified to achieve a temperature homogeneity of ±3°C along the 7.15 m long coil during temperature plateaus at 210°C, 400°C and 665°C. For this purpose, the furnace provides the control of 16 heating zones. In order to further optimize furnace control parameters a manual correction of plateau times was carried out. The implemented automatic homogeneity function on the furnace will be used at a later stage to automatically control the plateau times. First RHT cycles have been performed on MQXFB copper practise coils mounted inside a reaction fixture. This allowed to fine tune setting parameters and to cope with the RHT specified in Table V. For the monitoring of the temperatures the implemented 40 thermocouples (N type) were equally distributed on the reaction fixture and the surrounding gas volume. Figure 5 presents the programmed RHT set temperature and the evolution of the averaged measured temperatures of the thermocouples mounted on the reaction fixture over time. Boost steps were programmed in the RHT cycle to reach the plateaus in reduced time. They were adjusted in order to minimize a temperature overshoot on the reaction

TABLE V
MQXF REACTION HEAT TREATMENT SPECIFICATION

| TRAMP (°C) | RATE (°C/H) | TDWELL (°C) | PLATEAU (H) | HOMOGEINITY (°C) |
|---|---|---|---|---|
| 20-210 | 25 | 210 | 48 | ±3 |
| 210-400 | 50 | 400 | 48 | ±3 |
| 400-665 | 50 | 665 | 72 | ±3 |
| 665-20 | -25 | | | |

fixture. Additionally the ramp rate and the temperature homogeneity of the thermocouples mounted on the reaction fixture are shown. Results of the data analysis of the executed

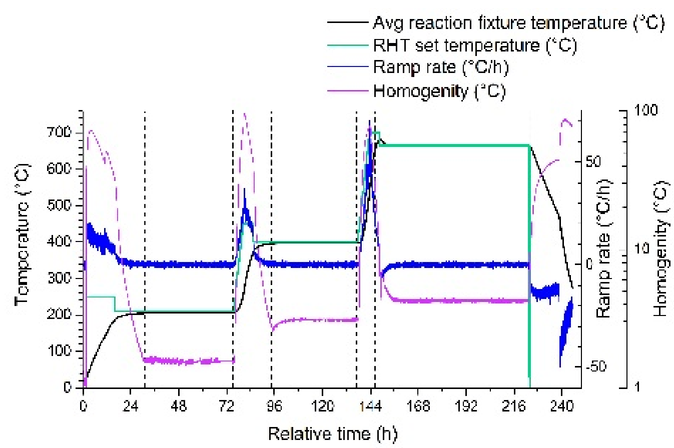


Fig. 5. Reaction heat treatment test on a MQXFB copper practise coil performed on the 7 Dec. 2016. RHT set temperature and averaged reaction fixture temperature versus time, ramp rate versus time and reaction fixture temperature homogeneity versus time.

TABLE VI
SUMMARY OF THE COPPER COIL TEST
DWELL TIMES

| Temperature (°C) | Plateau (h) | Homogeneity (°C) | $\overline{T}_{tooling}$ (°C) | $\overline{T}_{gas}$ (°C) |
|---|---|---|---|---|
| 210 | 43 | 1.5 | 206.5 | 206.4 |
| 400 | 44 | 3.1 | 397.1 | 397.1 |
| 665 | 77 | 4.7 | 664.1 | 664.1 |

RAMPING TIME AND RATE

| Ramp (°C) | Plateau (h) | Rate (°C/h) | max(Rate) (°C/h) |
|---|---|---|---|
| 20-210 | 30 | 6.0 | 25.4 |
| 210-400 | 18 | 10.5 | 41.0 |
| 400-665 | 9 | 28.7 | 70.6 |
| 665-270 | 22 | -18.2 | -51.1 |

RHT are summarized in Table VI. The dwell times at 210°C and 400°C were maintained slightly too short with 43 h and 44 h respectively in comparison to 48 h specified. On the contrary, the 665°C dwell time was maintained 5 h longer than specified, whereas the temperature homogeneity was lower than the specified ±3°C. The averaged heating rates of all ramps were below specified values, the maxima are however exceeding the specified values. Further test were performed with low-grade $Nb_3Sn$ coils (CR102 & CR103). The ramping times of the $Nb_3Sn$ coil increased in comparison to the copper dummy coil, the achieved homogeneity has remained below the specification values.

## V. Vacuum impregnation

The vacuum impregnation system and process were previously described for the 11T dipole coils [10]. The similar process for the MQXFB coil impregnation is carried out on the same system inside LMF. Before the impregnation the splicing operation of the $Nb_3Sn$ to Nb-Ti joints is prepared on the inner and outer layer. The $Sn_{96}Ag_4$ alloy and the MOB39 flux are used for soldering. A picture of the heating mould as well as the soldering heat cycle are shown in Figure 6. The spring loaded support allows to apply uniform pressure on the leads in order to achieve the required soldering quality and low splice resistance. Currently the resistance values are measured to be below 100 μΩ. The definition of the RT resistance (RRT) acceptance criteria is under development. The procedure of the impregnation process starts by cutting and cleaning the quench heaters. The coil is transferred into the impregnation fixture and

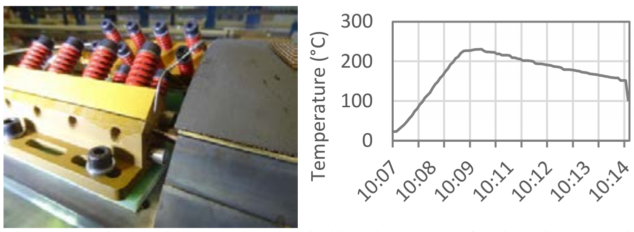


Fig. 6. Left : Resistive spring-loaded heating mould for the $Nb_3Sn$ to Nb-Ti lead cables; Right: Thermal cycle for splicing the $Nb_3Sn$ to Nb-Ti lead cables.

the outer layer quench heater is installed allowing to carry out all necessary electrical connection to voltage taps. The quench heater is afterwards covered with three layers of Hexcel 4522 fibre glass with a total thickness of 390 µm. A radial 40 µm Teflon coated seal-foil provides the interface to the inner radial wall of the impregnation cavity. The Teflon allows demoulding after the process. Afterwards the fixture is rotated to allow the quench heater installation and the placement of a single Hexcel 4522 insulation layer. Prior the transfer to the vacuum impregnation system a leak test is carried out with gaseous nitrogen at 2.5 bars for 20 min. Since the leak rate computation requires a precise definition of the volume the acceptance criteria was set to a pressure loss of 30 mbar during test duration. The heating system for the resin polymerization is assembled on the conveyor table of the impregnation mould and consists of 12 heating plates with a total power of 2 kW. The anhydride epoxy system CTD-101K with a maximum pot life of 20 hours from the Composite Technology Development company is used as impregnation resin. For the impregnation a single connection point between the resin mixer and impregnation fixture is used. Prior the process the fixture is inserted into the vacuum chamber, afterwards the chamber is lifted on one side resulting in an angle of 18°. A heating to 110°C allows to outgas residuals which are iteratively flushed with Nitrogen. The resin injection is carried out at 60°C and under a vacuum level to better than 5 x $10^{-2}$ mbar. Figure 7 presents the temperature tracking of the injection and polymerization monitored by type K thermocouples. The peristaltic pumps which are used to inject the resin are stopped once the resin has reached the outlet of the impregnation fixture. This takes about 45 min and is followed by ramping the temperature to 110°C where a plateau of 5 h allows the gelling of the resin. The so called post curing process is sunsequently carried out at 125°C at a plateau time of 16 h. After the

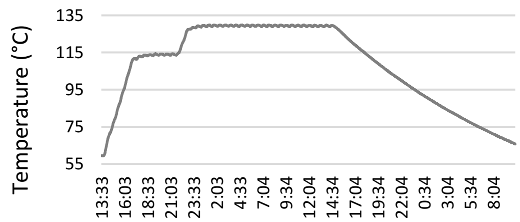


Fig. 7. Polymerization cycle after finalization of resin injection..

successful polymerization the mould is being extracted from the vacuum chamber and transferred into the winding zone for mould opening and cleaning of resin residuals. To monitor the quality of resin injection and polymerization a capacitive measurement method was developed and is currently tested throughout the impregnation process of 11T and MQXFB coils [11]. The aim is to quantify the status of impregnation and potentially further optimization of the polymerization cycle.

## VI. Status on iinfrastructure for the prototype assembly

In 2016 the development and procurement of the magnet assembly tooling was launched. The tooling concepts were taken from US-LARP Q2 [12] and the CERN short model assembly [13, 14]. Specific adaptations with respect to the length, alignment and implementation inside the LMF infrastructure were applied. The tooling will allow to perform the following assembly steps:

- Ground insulation forming
- Ground insulation installation
- Coil-pack assembly
- Coil-pack and yoke assembly bench
- Yoke and shell assembly
- Coil rotation
- Coil pack lifting girder
- High pressure system for bladder and key operation

The assembly tooling delivery will start in the last quarter of 2017 followed by the installation, alignment and commissioning inside the LMF. The two main tooling for the magnet assembly are shown in Figure 8. The coil pack assembly bench allows to rotate and assemble the Al collars and

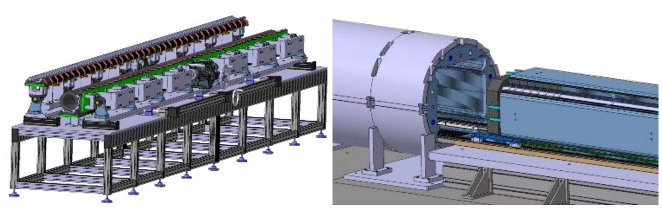

Fig. 8. 3d-design of the coil pack assembly bench (left) and a view of the interface of the coil-pack insertion tool into the yoke-shell assembly (right).

the iron pads on the pre-assembled coils. The coil pack is then inserted into the pre-assembled yoke-shell cavity. The tooling commissioning will start in autumn 2017 and will be followed by an assembly test which will be based on the four full-length practice coils. A new tooling was developed to carry out the ground insulation forming. The form stability is achieved by plastic deformation. Previously a forming mould and thermal treatment were required to achieve the required form stability. Figure 9 is shows the developed mockup of the insulation forming tool.

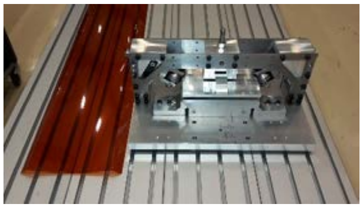

Fig. 9. Mock-up of the ground insulation forming tooling.

## VII. Quality assurance

In order to ensure repeatability and good documentation, the quality measures and documentation developed for the production of the LHC main dipoles and also during the LHC shutdown 1 are applied under the supervision and support of LMF QA team. Working procedures for all production steps were written and iteratively improved throughout the practise coil fabrication. Also workspace and machine safety are controlled with respect to the procedures and development of the production process [15].

## VIII. Coil production outlook

During this prototyping phase a total of 12 full performance $Nb_3Sn$ coils will be produced. The production of the coils for the first prototype assembly has been started in 2017. The schedule requires to finalize the four coils in early 2018 followed by the prototype assembly. A commissioning and validation test of all assembly tooling will be launched in late autumn 2017. A mandatory step before the assembly of the prototype will be the validation test based on practise coils under fully representative conditions. The four practise coils will be available already in October 2017. Therefore it is crucial that the installation of all necessary tooling is launched in parallel to the ongoing prototype coil production. The work on the validation test will be launched in September 2017 by the yoke and shell module assembly.

## IX. Conclusion

A status about the long MQXFB coil fabrication has been presented. The focus of the paper was put on the electrical and geometrical qualification measurements. The optimization of the titanium pole gap distribution was presented. It has allowed to achieve a closed pole gap after the reaction heat treatment. In addition information on the electrical test procedure has been provided. These tests are carried out after each manufacturing step and allow to provide a measure for the insulation performance. The analysis of the first RHT was presented. The analysis has allowed to further optimize temperature homogeneity and plateau times. The ramping times still remain below the specified 50°C/h which is related to the linear mass of the reaction fixture. An overview about the successful coil impregnation process was presented. Three long coils were impregnated so far, electrical qualification tests carried out on the low performance coils have indicated the robustness of the resin insulation. The procurement of tooling for the prototype magnet assembly has been launched. The two main assembly benches were introduced and a new concept for the ground insulation tooling presented. The production outline aims to a first functional and full performance prototype assembly in the first quarter of 2018. Except the unfortunate loss of the first full performance coil CR103 after RHT no show-stoppers were identified for allowing successful continuation of the MQXFB magnet fabrication.

## Acknowledgment

We are grateful to the CERN central workshop team for their help in the procurement of the tooling for the prototype assembly. In addition we would like to thank the CERN design office for their major contribution to the tooling design.

## References

[1] [1] "HL-LHC Preliminary Design Report", CERN-ACC-2014-0300, 28 November 2014.

[2] [2] S. Feher, *et al*., "Production and Installation of the LHC Low-β Triplets," *IEEE Trans. Appl. Supercond.,* vol. 16, no. 2, pp. 437-440, June 2006.

[3] [3] A. Yamamoto, *et al*., "Production and Measurement of the MQXA Series of LHC Low-β Insertion Quadrupoles", *IEEE Trans. Appl. Supercond.,* vol. 15, no. 2, pp. 1084-1089, June 2005.

[4] [5] E. Todesco, *et al.,* "Design Studies for the Low-Beta Quadrupoles for the LHC Luminosity Upgrade," *IEEE Trans. Appl. Supercond.*, vol. 23 no. 3, pp. 4002405, June 2013.

[5] [6] E. Todesco, *et al.,* "A first baseline for the magnets in the high luminosity LHC insertion regions," *IEEE Trans. Appl. Supercond.*, vol. 24 no. 3, pp. 4003305, June 2014.

[6] P. Ferracin, et al., "Fabrication and Test of a 3.7 m Long Support Structure for the LARP $Nb_3Sn$ Quadrupole Magnet LQS01," IEEE Trans. Appl. Supercond., vol. 19, no. 3, pp. 1683-1686, June 2009.

[7] J. Ferradas Troitino *et al.*, "Applied metrology in the production of Applied metrology in the production of superconducting model magnets for particle superconducting model magnets for particle accelerators", *IEEE Trans. Appl. Supercond.*, submitted for publication.

[8] F. Lackner et al., "Status of the Long MQXFB $Nb_3Sn$ Coil Prototype Production for the HiLumi LHC", *IEEE Trans. Appl. Supercond.*, vol. 27, no. 4, Jun. 2017

[9] F. Lackner *et al*., "Analysis of temperature uniformity during heat treatment of $Nb_3Sn$ coils for the High Luminosity LHC superconducting magnets," *IEEE Trans. Appl. Supercond.*, vol. 26, no. 4, Jun. 2016

[10] F. Savary et Al., "The 11 T Dipole for HL-LHC: Status and Plan *", IEEE Transactions on Applied Superconductivity*, vol. 26, issue 4, 2016, ISSN 1051- 8223.

[11] A. Foussat *et al.*, "Frequency domain Diagnosis Methods for Quality Assessment of $Nb_3Sn$ coil Insulation systems and impedance measurement", *IEEE Trans. Appl. Supercond.*, submitted for publication.

[12] G. Ambrosio, "$Nb_3Sn$ High Field Magnets for the High Luminosity LHC Upgrade Project," IEEE Trans. Appl. Supercond., vol. 25 no. 3, pp. 4002107, June 2015.

[13] M. Juchno, "Support Structure Design of the $Nb_3Sn$ Quadrupole for the High Luminosity LHC," *IEEE Trans. Appl. Supercond.*, vol. 25 no. 3, pp. 4001804, June 2015.

[14] P. Ferracin et al., "Development of MQXF: The $Nb_3Sn$ Low-β Quadrupole for the HiLumi LHC," IEEE Trans. Appl. Supercond., vol. 26, no. 4, pp. 4000207, June 2016.

[15] R. Principe *et al*., "Quality Assurance of the 13-kA Superconducting Magnet Circuits Consolidation of the LHC at CERN," in *IEEE Transactions on Applied Superconductivity*, vol. 26, no. 4, pp. 1-5, June 2016. doi: 10.1109/TASC.2016.2528044